References

[1] Adams JC, Watt FM. Regulation of development and differentiation by the extracellular matrix. Development 1993;117:1183–98.

[2] Peterson WJ, Tachiki KH, Yamaguchi DT. Extracellular matrix alters the relationship between thymidine incorporation and proliferation of MC3T3-E1 cells during osteogenesis in vitro. Cell Prolif 2002;35:9–22.

[3] Langer R, Vacanti JP. Tissue engineering. Science 1993;260:920–6.

[4] Mooney DJ, Mikos AG. Growing new organs. Sci Am 1999;280:38–43.

[5] Hori Y, Nakamura T, Matsumoto K, Kurokawa Y, Satomi S, Shimizu Y. Tissue engineering of the small intestine by acellular collagen sponge scaffold grafting. Int J Artif Organs 2001;24:50–4.

[6] Yamamoto M, Takahashi Y, Tabata Y. Controlled release by biodegradable hydrogels enhances the ectopic bone formation of bone morphogenetic protein. Biomaterials 2003;24:4375–83.

[7] Gamez E, Ikezaki K, Fukui M, Matsuda T. Photoconstructs of nerve guidance prosthesis using photoreactive gelatin as a scaffold. Cell Transplant 2003;12:481–90.

[8] Lavik E, Teng YD, Snyder E, Langer R. Seeding neural stem cells on scaffolds of PGA, PLA, and their co-polymers. Method Mol Biol 2002;198:89–97.

[9] Lieb E, Tessmar J, Hacker M, Fischbach C, Rose D, Blunk T, Mikos AG, Gopferich A, Schulz MB. Poly(D,L-lactic acid)-poly(ethylene glycol)-monomethyl ether diblock copolymers control adhesion and osteoblastic differentiation of marrow stromal cells. Tissue Eng 2003;9:71–84.

[10] Shin M, Ishii O, Sueda T, Vacanti JP. Contractile cardiac grafts using a novel nanofibrous mesh. Biomaterials 2004;25:3717–25.

[11] Alsberg E, Anderson KW, Albeiruti A, Rowley JA, Mooney DJ. Engineering growing tissues. Proc Nat Acad Sci 2002;99:12025–30.

[12] Chang CH, Liu HC, Lin CC, Chou CH, Lin FH. Gelatin-chondroitin-hyaluronan tri-copolymer scaffold for cartilage tissue engineering. Biomaterials 2003;24:4853–8.

[13] Tsuchida E, Abe K. Interactions between macromolecules in solution and intermacromolecular complexes. Adv Polym Sci 1982;45:1–119.

[14] Hamano T, Teramoto A, Iizuka E, Abe K. Effects of polyelectrolyte complex (PEC) on human periodontal ligament fibroblasts (HPLF) function. I. Three-dimensional structure of HPLF cultured PEC. J Biomed Mater Res 1998;41:257–69.

[15] Hamano T, Teramoto A, Iizuka E, Abe K. Effects of polyelectrolyte complex (PEC) on human periodontal ligament fibroblasts (HPLF) function. II. Enhancement of HPLF differentiation and aggregation on PEC by *L*-ascorbic acid and dexamethasone. J Biomed Mater Res 1998;41:270–7.

[16] Hamano T, Chiba D, Nakatsuka K, Nagahata M, Teramoto A, Kondo Y, Hachimori A, Abe K. Evaluation of a polyelectrolyte complex (PEC) composed of chitin derivatives and chitosan, which promotes the rat calvarial osteoblast differentiation. Polym Adv Technol 2002;13:46–53.

[17] Maio AD, Vaga VL, Contreras JE. Gap junctions, homeostasis, and injury. J Cell Physiol 2002;191:269–82.

[18] Tsuchiya T, Hata H, Nakamura A. Studies on the tumor-promoting activity of biomaterials: inhibition of metabolic cooperation by polyetherurethane and silicone. J Biomed Mater Res 1995;29:113–9.

[19] Tsuchiya T, Takahara A, Cooper SL, Nakamura A. Studies on the tumor-promoting activity of polyurethanes: depletion of inhibitory action of metabolic cooperation on the surface of a polyalkyleneurethane but not a polyetherurethane. J Biomed Mater Res 1995;29:835–41.

[20] Nakaoka R, Tsuchiya T, Sakaguchi K, Nakamura A. Studies on in vitro evaluation for the biocompatibility of various biomaterials: inhibitory activity of various kinds of polymer microspheres on metabolic cooperation. J Biomed Mater Res 2001:279–84.

[21] Nakaoka R, Tsuchiya T, Nakamura A. The inhibitory mechanism of gap junctional intercellular communication induced by polyethylene and the restorative effects by surface modification with various proteins. J Biomed Mater Res 2001;57:567–74.

[22] Nagahata M, Tsuchiya T, Ishiguro T, Matsuda N, Nakatsuchi Y, Teramoto A, Hachimori A, Abe K. A novel function of *N*-cadherin and connexin 43: marked enhancement of alkaline phosphotase activity in rat calvarial osteoblast exposed to sulfated hyaluronan. Biochem Biophys Res Commun 2004;315:603–11.

[23] Tamada Y, Ikada Y. Fibroblast growth on polymer surfaces and biosynthesis of collagen. J Biomed Mater Res 1994;28:783–9.

[24] Ohyama M, Suzuki N, Yamaguchi Y, Maeno M, Otsuka K, Ito K. Effect of enamel matrix derivative on the differentiation of C2C12 cells. J Periodontol 2002;73:543–50.

[25] Wade MH, Trosko JE, Schlindler M. A fluorescence photobleaching assay of gap junctional-mediated communication between human cells. Science 1986;232:525–8.

[26] Kato S, Akagi T, Sugimura K, Kishida A, Akashi M. Evaluation of biological responses to polymeric biomaterials by RT-PCR analysis IV: study of c-myc, c-fos and p53 mRNA expression. Biomaterials 2000;21:521–7.

[27] Tanahashi M, Matsuda T. Surface functional group dependence on apatite formation on self-assembled monolayers in a simulated body fluid. J Biomed Mater Res 1997;34:305–15.

[28] Matsuda N, Horikawa M, Yoshida M, Watanabe M, Nagahata M, Teramoto A, Abe K. Enhanced DNA synthesis accompanied by constitutive phosphorylation of the ERK pathway in human fibroblasts cultured on a polyelectrolyte complex. Biomaterials 2003;24:4771–6.

TISSUE ENGINEERING
Volume 11, Number 9/10, 2005

Enhancement of Gap Junctional Intercellular Communication of Normal Human Dermal Fibroblasts Cultured on Polystyrene Dishes Grafted with Poly-*N*-isopropylacrylamide

TSUTOMU NAGIRA, Ph.D.,[1,2] SUSAN BIJOO MATTHEW, Ph.D.,[1] YOKO YAMAKOSHI, Ph.D.,[3] and TOSHIE TSUCHIYA, Ph.D.[1]

ABSTRACT

Technology developed to allow recovery of cells without enzyme treatment, involving a dish grafted with a thermoreactive polymer gel of poly-*N*-isopropylacrylamide (PIPAAm), was found to significantly enhance gap junctional intercellular communication (GJIC) in normal human dermal fibroblasts (NHDF cells). NHDF cells were cultured for 4 days on PIPAAm-grafted dishes irradiated with various doses of electron beams, and GJIC was assayed by the scrape-loading dye transfer method. The area of dye transfer was greater in the PIPAAm-grafted dishes than in the control culture dishes, indicating that the PIPAAm-grafted dishes enhanced the GJIC of NHDF cells. Connexin-43 (Cx43) expression was analyzed because Cx43 is considered to be a main component of the gap junctional channel. PIPAAm-grafted dishes irradiated with 100, 250, or 500 kGy of electron beams showed significantly enhanced expression of Cx43-NP, Cx43-P1, and especially Cx43-P2. Enhanced expression of Cx43-P2, a functional transmembrane protein, may be related to the promotion of GJIC. These results suggest that the PIPAAm-grafted dish not only enables the enzyme-free recovery of a cell monolayer for use in the construction of a three-dimensional artificial tissue, but also significantly contributes to the enhancement of GJIC, which may partly promote tissue strength on the surface of the PIPAAm-grafted dish.

INTRODUCTION

GAP JUNCTIONS exist on the cell membrane and work as intercellular channels that allow the exchange of substances with molecular masses up to 1 kDa, such as ions, sugars, and amino acids, by the function called gap junctional intercellular communication (GJIC).[1–3] Gap junctions are constructed from transmembrane proteins, called connexins,[4,5] that form a hemichannel, called a connexon. GJIC is suggested to be well correlated with passage of metabolites,[6] cell proliferation,[7] and cell differentiation[8]; thus, enhancement of the function of the gap junction is supposed to be important in the differentiation of engineered tissue products, such as those involving heart cells.[9–11] Poly-*N*-isopropylacrylamide (PIPAAm)-grafted dishes, which were originally developed as a thermosensitive scaffold for cell culture, are useful to maintain the GJIC of tissues cultured on them because they do not require enzyme treatment, which destroys connexins.[12–14]

PIPAAm is a thermoresponsive polymer that has a low critical solution temperature of 32°C: hydrated PIPAAm

[1]Division of Medical Devices, National Institute of Health Sciences, Tokyo, Japan.
[2]Japan Association for the Advancement of Medical Equipment, Tokyo, Japan.
[3]Center for Polymers and Organic Solids, Department of Chemistry and Biochemistry, University of California, Santa Barbara, Santa Barbara, California.

has an extended chain conformation below 32°C and dehydrated PIPAAm has a collapsed chain conformation above 32°C.[15–27] This property of PIPAAm has been exploited in intelligent materials for drug delivery systems and chromatography technology.[16–23] The PIPAAm-grafted dish has been found to enable the recovery of cell monolayers easily without enzyme treatment because cells cannot adhere to a hydrophilic surface below 32°C.[24–26] Cell monolayers are the basic units used to construct three-dimensional tissues *in vitro*. Because a cell monolayer recovered without enzyme treatment maintains normal adhesive and junctional proteins, it can easily adhere to the other tissues or cell sheets to construct a three-dimensional artificial tissue.[27–29] Thus, the PIPAAm-grafted dish has the potential to enable the development of new techniques in tissue engineering.

Although the PIPAAm-grafted dish has made a new era in tissue engineering possible, its effects on connexin-43 (Cx43) expression and GJIC have not been studied well. These effects are important because Cx43 plays an important role in cell proliferation and cell differentiation.

In this study, GJIC and expression of Cx43 molecules were examined by scrape-loading dye transfer (SLDT) assay[30] and Western blotting, respectively, using NHDF cells cultured on PIPAAm-grafted dishes irradiated with various doses of electron beams in order to clarify the safety and appropriateness of this material for the culture of artificial cultured tissues.

MATERIALS AND METHODS

Materials

N-isopropylacrylamide monomer (NIPAAm) was purchased from Wako Pure Chemical Industries (Osaka, Japan). Isopropyl alcohol was obtained from Dojindo (Kumamoto, Japan), and Lucifer yellow dye was from Molecular Probes (Eugene, OR).

Cell culture

Normal human dermal fibroblasts (NHDF cells; Sanko Junyaku, Tokyo, Japan) were cultured in Dulbecco's modified Eagle's medium (GIBCO DMEM; Invitrogen, San Diego, CA), supplemented with 10% heat-inactivated fetal calf serum (FCS; Invitrogen) and antibiotics (penicillin [100 units/mL]-streptomycin [100 units/mL]) (Invitrogen) at 37°C. NHDF cells were maintained in a humidified atmosphere of 5% CO_2 and 95% air.

Preparation of PIPAAm-grafted culture dishes

One hundred microliters of 40% NIPAAm dissolved in isopropyl alcohol was added to 35-mm dishes and irradiated with various doses of electron beams (25, 100, 250, or 500 kGy), using an area electron beam-processing system (Nissin High Voltage, Kyoto, Japan). The PIPAAm-grafted dishes were then rinsed three times with ice-cold sterile water (2 ml) for 5 min, sealed, and dried under vacuum.

Cell morphology

NHDF cells were cultured on control and PIPAAm-grafted dishes. Confluent cells (after 4 days of culture) were fixed with formalin solution, stained with 3% Giemsa solution, and observed with an optical microscope.

Protein assay

The protein concentration of cells cultured on control and PIPAAm-grafted dishes was measured with a bicinchoninic acid (BCA) protein assay kit (Pierce Biotechnology, Rockford, IL). Ten-microliter cell samples were

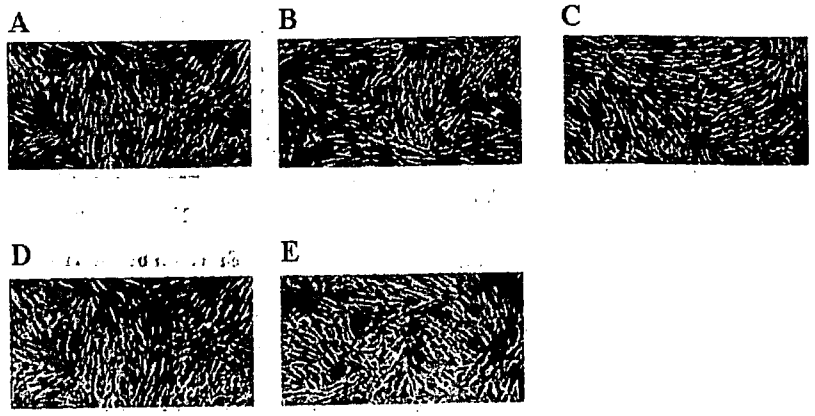

FIG. 1. Optical microscopy images of NHDF cells cultured on PIPAAm-grafted dishes. NHDF cells were cultured for 4 days on PIPAAm-grafted dishes prepared by irradiation with various doses of electron beams (0, 25, 100, 250, or 500 kGy). (**A**) Non-irradiated; (**B**) 25-kGy electron beam; (**C**) 100-kGy electron beam; (**D**) 250-kGy electron beam; (**E**) 500-kGy electron beam.

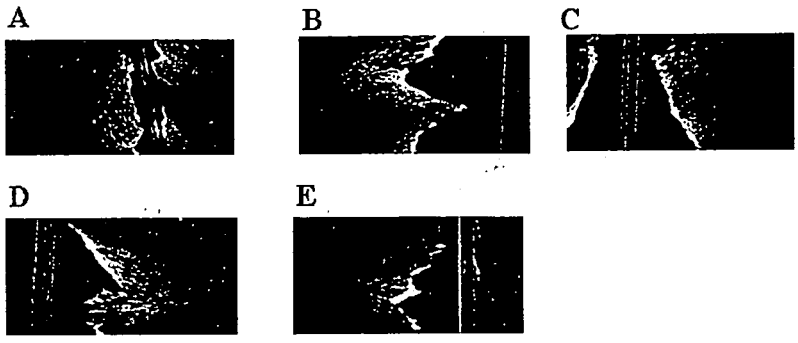

FIG. 2. Fluorescence of NHDF cells by SLDT assay. Transmission of Lucifer yellow into NHDF cells cultured on PIPAAm-grafted dishes irradiated with various doses of electron beams was detected 5 min after scrape-loading. (**A**) Nonirradiated; (**B**) 25-kGy electron beam; (**C**) 100-kGy electron beam; (**D**) 250-kGy electron beam; (**E**) 500-kGy electron beam.

added to 200 μL of the working solution and incubated at 37°C for 30 min in a 96-well plate. Absorbance was then measured at 562 nm in accordance with the manufacturer's protocols.

Scrape-loading dye transfer assay

NHDF cells were seeded on control and PIPAAm-grafted dishes at a density of 1×10^5 cells/mL and cultured for 4 days to form a confluent monolayer. Confluent NHDF cells were washed three times with phosphate-buffered saline containing Ca^{2+} and Mg^{2+} [PBS(+)], and the cell monolayer was scraped with a surgical blade. Fluorescent dye (Lucifer yellow; MW 457.2) at a concentration of 0.1% in PBS(+) was added.[30,31] Cells were exposed to the dye at 37°C for 5 min, and then the dye was discarded and the cells were washed four times with PBS(+). The distance that the dye had migrated was measured under a fluorescence microscope equipped with a type UFX-DXII CCD camera and super high-pressure mercury lamp power supply (Nikon, Tokyo, Japan). The dye migration was measured from the cut edge of the scrape to the edge of the dye front in the cells that were visually detectable.[30]

Western blotting

NHDF cells were cultured for 4 days. After being washed with ice-cold PBS(–) three times, the cells were lysed in 500 μL of lysis buffer (50 mM Tris-HCl [pH 6.8] containing 150 mM NaCl, 5 mM EDTA, 0.1 mM leupeptin, 1 mM phenylmethylsulfonyl fluoride, and 1% Nonidet P-40) for 30 min on ice with shaking. The cell lysates were centrifuged (10,000 rpm) at 4°C for 20 min, and the supernatants were collected. The protein concentrations of the lysates were determined by BCA assay.

Equivalent amounts of protein sample were applied to 12% sodium dodecyl sulfate (SDS)–polyacrylamide gels and then transferred to a nitrocellulose membrane at 120 V for 60 min. The membrane was blocked with Block Ace (Yukijirusi, Tokyo, Japan) overnight at 4°C. After being washed for 30 min in PBS with 0.05% Tween 20, the membrane was incubated for 2 h with anti-Cx43 polyclonal antibody [diluted 1:1000 in PBS(–) with 0.05% Tween 20; Zymed Laboratories, South San Francisco, CA], followed by incubation with horseradish peroxidase (HRP)-conjugated goat anti-rabbit IgG secondary antibody (diluted 1:5000; Zymed Laboratories). The image was visualized with an enhanced chemiluminescence (ECL) detection kit (Amersham Biosciences/GE Healthcare, Little Chalfont, UK).

Statistical analysis

Significant differences between groups were evaluated by Student t test. Mean differences were considered significant when $p < 0.05$.

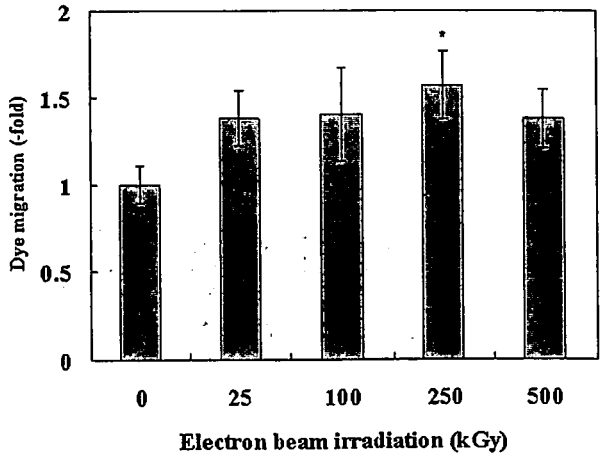

FIG. 3. Positive dye transfer in NHDF cells cultured on PIPAAm-grafted dishes. Transmission of Lucifer yellow was detected 5 min after scrape-loading in NHDF cells cultured on PIPAAm-grafted dishes irradiated with various electron beam doses (0, 25, 100, 250, or 500 kGy). Values represent means ± SD for three dishes. *Significant difference compared with control at $p < 0.05$ by t test.

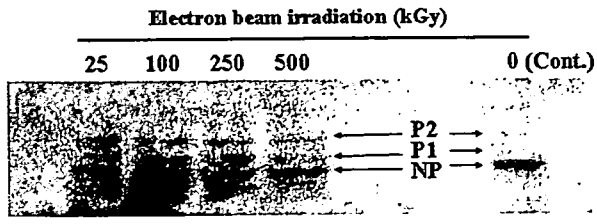

FIG. 4. Western blot of Cx43-NP, Cx43-P1, and Cx43-P2 expression; lysates of NHDF cells cultured on PIPAAm-grafted dishes irradiated with various doses of electron beams (0, 25, 100, 250, or 500 kGy) were applied to SDS–polyacrylamide gels. Fractionated proteins in the gels were transferred to nitrocellulose membrane and immunoblotted with anti-Cx43 polyclonal antibody as described in Material and Methods. Images of Cx43 on Western blot were captured with an Image scanner and analyzed with NIH Image software.

RESULTS

The appearance of NHDF cells grown on PIPAAm-grafted dishes irradiated with various doses of electron beams are shown in Fig. 1. No significant differences were observed by optical microscopy analysis between cells grown in dishes irradiated with various doses of electron beams. These results suggest that PIPAAm-grafted dishes are not toxic to NHDF cells.

The SLDT assay showed that dye migration in cells cultured on PIPAAm-grafted dishes irradiated with electron beams (25, 100, or 500 kGy) was enhanced by about 1.4-fold compared with that on control dishes. Interestingly, the dye migration in cells cultured on PIPAAm-grafted dishes irradiated with the 250-kGy electron beam was particularly enhanced, about 1.6 times higher than that on control dishes (Figs. 2 and 3). These results suggested that the GJIC of NHDF cells cultured on PIPAAm-grafted dishes was enhanced and that the GJIC on PIPAAm-grafted dishes irradiated with the 250-kGy electron beam was affected the most.

To further elucidate the effects of the PIPAAm grafting of culture dishes on GJIC, we analyzed the expression of Cx43, a transmembrane protein involved in GJIC. There are three forms of Cx43: Cx43-NP (nonphosphorylated Cx43), Cx43-P1 (monophosphorylated Cx43), and Cx43-P2 (another phosphorylated Cx43); Cx43-P2 is the most important and functional protein involved in GJIC. The results of Western blotting showed that the expression of Cx43-P1 and Cx43-P2 in NHDF cells cultured on PIPAAm-grafted dishes irradiated with 25, 100, 250, or 500 kGy of electron beams was considerably enhanced. Further, NHDF cells cultured on PIPAAm-grafted dishes irradiated with 100, 250, or 500 kGy of electron beams showed enhanced Cx43-NP expression (Figs. 4 and 5A). The Cx43-P2 expression of cells cultured on PIPAAm-grafted dishes irradiated with the 250-kGy electron beam dose showed the highest value, about 46% higher than that of control dishes. Cells cultured on PIPAAm-grafted dishes irradiated with electron beam doses of 25, 100, and 500 kGy were shown to have enhanced total Cx43 expression. Cells cultured on PIPAAm-grafted dishes irradiated with 100- and 250-kGy electron beam doses showed the highest total Cx43 expression, about 36.6% higher than that of control dish (Fig. 5B).

The Cx43-P2 expression of NHDF cells cultured on PIPAAm-grafted dishes irradiated with 25, 100, 250, and 500 kGy correlated well with GJIC ($R^2 = 0.9398$).

DISCUSSION

Thermoresponsive PIPAAm-grafted dishes irradiated with electron beams have been used to culture cell monolayers because the monolayers can be recovered without enzyme treatment, making PIPAAm a useful material for tissue engineering.

It has been reported that junctional proteins, cellular adherence proteins on the cell membrane, interact via

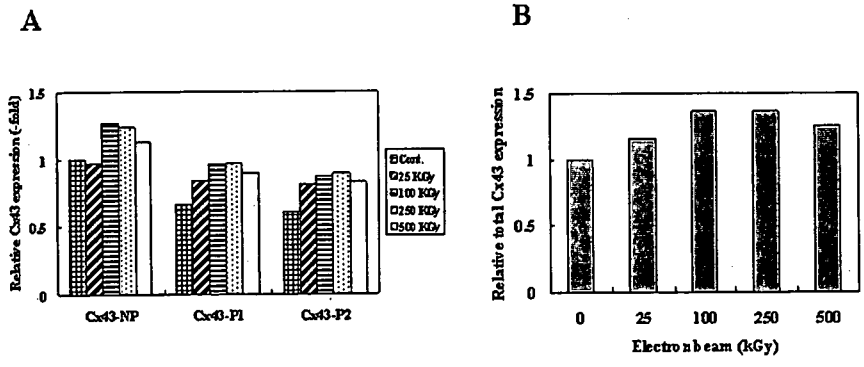

FIG. 5. Relative expression levels of Cx43-NP, Cx43-P1, and Cx43-P2 (A) and relative expression levels of total Cx43 (NP+P1+P2) (B) of NHDF cells cultured on PIPAAm-grafted dishes irradiated with various doses of electron beams (0, 25, 100, 250, or 500 kGy).

GJIC.[31] In this study, an SLDT assay demonstrated that dye migration in cultured NHDF cells was significantly enhanced in all PIPAAm-grafted dishes tested. Therefore, the chemical structure of the PIPAAm surface may stimulate junctional proteins on the cell membrane, and the stimulated junctional proteins may induce the enhancement of GJIC.

Cx43 expression of NHDF cells cultured on PIPAAm-grafted dishes irradiated with a 250-kGy electron beam changed significantly. Structural differences in PIPAAm triggered by the 250-kGy electron beam induced Cx43 protein expression by NHDF cells, probably by affecting the gene expression of NHDF cells. Further, total Cx43 expression was shown to be enhanced in cells cultured on PIPAAm-grafted dishes irradiated with various doses of electron beams (25, 100, 250, or 500 kGy). Differences due to the electron beam dose should be studied further.

Although the mechanism involved was not determined, it has been reported that basic fibroblast growth factor (bFGF) and keratinocyte growth factor (KGF) enhance GJIC activity and the expression of Cx43.[32–35] If bFGF and KGF in FCS are adsorbed onto the PIPAAm surface, cells can efficiently access these growth factors from the PIPAAm surface, and GJIC may be enhanced. It is also reported that bFGF activates protein kinase A (PKA),[36] an important regulator of Cx43, promoting the phosphorylation of Cx43 and enhancing GJIC.[37] Therefore, bFGF adsorbed onto the PIPAAm surface may bind its receptor and induce the activation of PKA, resulting in an enhancement of GJIC on NHDF cells caused by the increase in Cx43-P2 band protein.

In the process of posttranslational change, Cx43-P2 becomes insoluble in Triton X-100.[38] Thus, not all Cx43-P2 may be included in the lysate, and some Cx43-P2 may have been included in the pellet. More Cx43-P2 may have existed than was detected in the present results obtained by Western blotting.

In this study, it was shown that the use of PIPAAm-grafted dishes irradiated with various doses of electron beams enhanced GJIC and Cx43 expression in cultured NHDF cells. This suggests that PIPAAm-grafted dishes may promote efficient tissue regeneration, because GJIC plays an important role in increasing tissue strength.[39]

ACKNOWLEDGMENTS

This work was supported in part by a Grant-in-Aid for Scientific Research on Advanced Medical Technology from the Ministry of Labor, Health, and Welfare, Japan and by a Grant-in-Aid from the Japan Human Sciences Foundation.

REFERENCES

1. Giaume, C., Tabernero, A., and Medina, J.M. Metabolic trafficking through astrocyte gap junctions. Glia **21,** 114, 1997.
2. Abdullah, K.M., Luthra, G., Bilski, J.J., Abdullah, S.A. Reynolds, L.P., Redmer, D.A., and Grazul-Bilska, A.T. Cell-to-cell communication and expression of gap junctional proteins in human diabetic and nondiabetic skin fibroblasts. Endocrine **10,** 35, 1999.
3. Grossman, H.B., Liebert, M., Lee, I.W., and Lee, S.W. Decreased connexin expression and intercellular communication in human bladder cancer cells. Cancer Res. **54,** 3062, 1994.
4. Vera, B., Sanchez-Abarca, L.I., Bolanos, J.P., and Medina, J.M. Inhibition of astrocyte gap junctional communication by ATP depletion is reversed by calcium sequestration. FEBS Lett. **392,** 225, 1996.
5. Bukauskas, F.F., Jordan, K., Bukauskiene, A., Bennett, M.V., Lampe, P.D., Laird, D.W., and Verselis, V.K. Clustering of connexin 43–enhanced green fluorescent protein gap junction channels and functional coupling in living cells. Proc. Natl. Acad. Sci. U.S.A. **97,** 2556, 2000.
6. Giaume, C., Tabernero, A., and Medina, J.M. Metabolic trafficking through astrocytic gap junctions. Glia **21,** 114, 1997.
7. Tabernero, A., Jimenez, C., Velasco, A., Giaume, C., and Medina, J.M. The enhancement of glucose uptake caused by the collapse of gap junction communication is due to an increase in astrocyte proliferation. J. Neurochem. **78,** 890, 2001.
8. Tsuchiya, T. A useful marker for evaluating tissue-engineered products: Gap-junctional communication for assessment of the tumor-promoting action and disruption of cell differentiation in tissue-engineered products. J. Biomater. Sci. Polym. Ed. **11,** 947, 2000.
9. Giaume, C., Marin, P., Cordier, J., Glowinski, J., and Premont, J. Adrenergic regulation of intercellular communications between cultured striatal astrocytes from the mouse. Proc. Natl. Acad. Sci. U.S.A. **88,** 5577, 1991.
10. Warn-Cramer, B.L., Cottrell, G.T., Burt, J.M., and Lau, A.F. Regulation of connexin-43 gap junctional intercellular communication by mitogen-activated protein kinases. J. Biol. Chem. **273,** 9188, 1998.
11. Shimizu, T., Yamato, M., Isoi, Y., Akutsu, T., Setomaru, T., Abe, K., Kikuchi, A., Umezu, M., and Okano, T. Fabrication of pulsatile cardiac tissue grafts using a novel 3-dimensional cell sheet manipulation technique and temperature-responsive cell culture surfaces. Circ. Res. **22,** e40, 2002.
12. Nandkumar, M.A., Yamato, M., Kushida, A., Konno, C., Hirose, M., Kikuchi, A., and Okano, T. Two-dimensional cell sheet manipulation of heterotypically co-cultured lung cells utilizing temperature-responsive culture dishes results in long-term maintenance of differentiated epithelial cell functions. Biomaterials **23,** 1121, 2002.
13. Kushida, A., Yamato, M., Kikuchi, A., and Okano, T. Two-dimensional manipulation of differentiated Madin–Darby canine kidney (MDCK) cell sheets: The noninvasive harvest from temperature-responsive culture dishes and transfer to other surfaces. J. Biomed. Mater. Res. **54,** 37, 2001.
14. Shimizu, T., Yamato, M., Akutsu, T., Shibata, T., Isoi, Y., Kikuchi, A., Umezu, M., and Okano, T. Electrically com-

municating three-dimensional cardiac tissue mimic fabricated by layered cultured cardiomyocyte sheets. J. Biomed. Mater. Res. **60,** 110, 2002.
15. Takezawa, T., Mori, Y., and Yoshizato, K. Cell culture on a thermo-responsive polymer surface. Biotechnology **8,** 854, 1990.
16. Chung, J.E., Yokoyama, M., Yamato, M., Aoyagi, T., Sakurai, Y., and Okano, T. Thermo-responsive drug delivery from polymeric micelles constructed using block copolymers of poly(*N*-isopropylacrylamide) and poly (butylmethacrylate). J. Control. Release **62,** 115, 1999.
17. Chung, J.E., Yokoyama, M., and Okano, T. Inner core segment design for drug delivery control of thermo-responsive polymeric micelles. J. Control. Release **65,** 93, 2000.
18. Kurisawa, M., Yokoyama, M., and Okano, T. Gene expression control by temperature with thermo-responsive polymeric gene carriers. J. Control. Release **69,** 127, 2000.
19. Kobayashi, J., Kikuchi, A., Sakai, K., and Okano, T. Aqueous chromatography utilizing pH-/temperature-responsive polymer stationary phases to separate ionic bioactive compounds. Anal. Chem. **73,** 2027, 2001.
20. Kikuchi, A., and Okano, T. Pulsatile drug release control using hydrogels. Adv. Drug Deliv. Rev. **54,** 53, 2002.
21. Kanazawa, H., Sunamoto, T., Ayano, E., Matsushima, Y., Kikuchi, A., and Okano, T. Temperature-responsive chromatography using poly (*N*-isopropylacrylamide) hydrogel-modified silica. Anal. Sci. **18,** 45, 2002.
22. Kobayashi, J., Kikuchi, A., Sakai, K., and Okano, T. Aqueous chromatography utilizing hydrophobicity-modified anionic temperature-responsive hydrogel for stationary phases. J. Chromatogr. A **958,** 109, 2002.
23. Yoshizako, K., Akiyama, Y., Yamanaka, H., Shinohara, Y., Hasegawa, Y., Carredano, E., Kikuchi, A., and Okano, T. Regulation of protein binding toward a ligand on chromatographic matrixes by masking and forced-releasing effects using thermoresponsive polymer. Anal. Chem. **74,** 4160, 2002.
24. Kikuchi, A., Okuhara, M., Karikusa, F., Sakurai, Y., and Okano, T. Two-dimensional manipulation of confluently cultured vascular endothelial cells using temperature-responsive poly(*N*-isopropylacrylamide)-grafted surfaces. J. Biomater. Sci. Polym. Ed. **9,** 1331, 1998.
25. Kushida, A, Yamato, M., Konno, C., Kikuchi, A., Sakurai, Y., and Okano, T. Temperature-responsive culture dishes allow nonenzymatic harvest of differentiated Madin–Darby canine kidney (MDCK) cell sheets. J. Biomed. Mater. Res. **51,** 216, 2000.
26. Shimizu, T., Yamato, M., Kikuchi, A., and Okano, T. Two-dimensional manipulation of cardiac myocyte sheets utilizing temperature-responsive culture dishes augments the pulsatile amplitude. Tissue Eng. **7,** 141, 2001.
27. Hirose, M., Yamato, M., Kwon, O.H., Harimoto, M., Kushida, A., Shimizu, T., Kikuchi, A., and Okano, T. Temperature-responsive surface for novel co-culture systems of hepatocytes with endothelial cells: 2-D patterned and double layered co-cultures. Yonsei Med. J. **41,** 803, 2000.
28. Yamato, M., Utsumi, M., Kushida, A, Konno, C., Kikuchi, A., and Okano, T. Thermo-responsive culture dishes allow the intact harvest of multilayered keratinocyte sheets without dispase by reducing temperature. Tissue Eng. **7,** 473, 2001.
29. Harimoto, M., Yamato, M., Hirose, M., Takahashi, C., Isoi, Y., Kikuchi, A., and Okano, T. Novel approach for achieving double-layered cell sheets co-culture: Overlaying endothelial cell sheets onto monolayer hepatocytes utilizing temperature-responsive culture dishes. J. Biomed. Mater. Res. **62,** 464, 2002.
30. el-Fouly, M.H, Trosko, J.E., and Chang, C.C. Scrape-loading and dye transfer: A rapid and simple technique to study gap junctional intercellular communication. Exp. Cell Res. **168,** 422, 1987.
31. Defamie, N., Mograbi, B., Roger, C., Cronier, L., Malassine, A., Brucker-Davis, F., Fenichel, P., Segretain, D., and Pointis, G. Disruption of gap junctional intercellular communication by lindane is associated with aberrant localization of connexin43 and zonula occludens-1 in 42GPA9 Sertoli cells. Carcinogenesis **22,** 1537, 2001.
32. Pepper, M.S., and Meda, P. Basic fibroblast growth factor increases junctional communication and connexin 43 expression in microvascular endothelial cells. J. Cell. Physiol. **153,** 196, 1992.
33. Nadarajah, B., Makarenkova, H., Becker, D.L., Evans, W.H., and Parnavelas, J.G. Basic FGF increases communication between cells of the developing neocortex. J. Neurosci. **18,** 7881, 1998.
34. Park, J.U., and Tsuchiya, T. Increase in gap junctional intercellular communication by high molecular weight hyaluronic acid associated with fibroblast growth factor 2 and keratinocyte growth factor production in normal human dermal fibroblasts. Tissue Eng. **8,** 419, 2002.
35. Doble, B.W., and Kardami, E. Basic fibroblast growth factor stimulates connexin-43 expression and intercellular communication of cardiac fibroblast. Mol. Cell. Biochem. **143,** 81, 1995.
36. Pursiheimo, J.P., Jalkanen, M., Tasken, K., and Jaakkola, P. Involvement of protein kinase A in fibroblast growth factor-2-activated transcription. Proc. Natl. Acad. Sci. U.S.A. **97,** 168, 2000.
37. Faucheux, N., Zahm, J.M., Bonnet, N., Legeay, G., and Nagel, M.D. Gap junction communication between cells aggregated on a cellulose-coated polystyrene: Influence of connexin 43 phosphorylation. Biomaterials **25,** 2501, 2004.
38. Musil, L.C., and Goodenough, D.A. Biochemical analysis of connexin43 intracellular transport, phosphorylation, and assembly into gap junctional plaques. J. Cell Biol. **115,** 1357, 1991.
39. Gutstein, D.E., Morley, G.E., Tamaddon, H., Vaidya, D., Schneider, M.D., Chen, J., Chien, K.R., Stuhlman, H., and Fishman, G.I. Conduction slowing and sudden arrhythmic death in mice with cardiac-restricted inactivation of connexin43. Circ. Res. **88,** 333, 2001.

Address reprint requests to:
Toshie Tsuchiya, Ph.D.
Division of Medical Devices
National Institute of Health Sciences
1-18-1 Kamiyoga
Setagaya-ku, Tokyo 158-8501, Japan

E-mail: tsuchiya@nihs.go.jp

J Artif Organs (2005) 8:184–191
DOI 10.1007/s10047-005-0302-3

ORIGINAL ARTICLE

Nasreen Banu, MD · Yasmin Banu, MD, PhD
Masamune Sakai, BSc · Tadahiko Mashino, PhD
Toshie Tsuchiya, PhD

Biodegradable polymers in chondrogenesis of human articular chondrocytes

Abstract The aim of this study was to evaluate the potential role of polyglycolic acid (PGA), poly(glycolic acid-ε-caprolactone) (PGCL), poly(L-lactic acid-glycolic acid) (PLGA), poly(L-lactic acid-ε-caprolactone, 75:25 (w/w)) [P(LA-CL)25], poly-ε-caprolactone (tetrabutoxy titanium) [PCL(Ti)], and fullerene C-60 dimalonic acid (DMA) in cartilage transplants. After 4 weeks of culture of human articular cartilage, the levels of cell proliferation and differentiation and the expression of cartilage-specific matrix genes were estimated. The relationship between cell differentiation and gap junction protein connexin 43 (Cx43) was also evaluated. All materials except PCL(Ti) retained cell proliferation activities similar to the controls. Cell differentiation levels from the highest to the lowest were in the following order: PGA >> PLGA > PGCL > Control = DMSO > P(LA-CL)25 = PCL(Ti) >> fullerene C-60 DMA. Expression of the collagen type II gene was selectively upregulated for PGA, PGCL, and PLGA and slightly increased for P(LA-CL)25 polymers but was downregulated for fullerene C-60 DMA. Aggrecan gene expression was strongest with PGA and was consistently expressed with other matrices, especially with PGCL and PLGA. However, the expression patterns of the connexin 43 gene were different from the former two genes. Multiple regression analysis revealed a high correlation between cartilage proteoglycans production and expression levels of these three genes.

Received: February 2, 2005 / Accepted: June 8, 2005

N. Banu · Y. Banu · T. Tsuchiya (✉)
Division of Medical Devices, National Institute of Health Sciences, 1-18-1 Kamiyoga, Setagaya-ku, Tokyo 158-8501, Japan
Tel. +81-3-3700-9196; Fax +81-3-3700-9196
E-mail: tsuchiya@nihs.go.jp

M. Sakai
Polymer Laboratory, UBE Industries, Ltd., Chiba, Japan

T. Mashino
Kyoritsu University of Pharmacy, Tokyo, Japan

The first two authors contributed equally to this work

Key words Human articular chondrocytes · Biodegradable polymers · Matrix gene · Connexin 43

Introduction

A shortage of donor tissue restricts the successful application of tissue reconstruction for various cartilage injuries. Tissue engineering is a relatively new and promising field directed at the evolution of new tissues that will offer hope to orthopedic patients with a variety of injuries. To permit repair of cartilage defects, many researchers are turning toward a tissue engineering approach involving cultured cells and biomaterials. Although these biomaterials, especially polyglycolic acid (PGA) and poly(L-lactic acid) (PLLA), play an increasingly important role in orthopedics, adverse reactions to these biomaterials have been reported in animal experiments. PLLA produces toxic substances due to acidic degradation,[1] and long-term implants of PLLA produced tumorigenicity in rats.[2] Despite these setbacks, numerous studies have documented the biocompatibility of these bioabsorbable polymers.[3–7] PLLA, PGA, and their copolymers also have been used in clinical practice.[5,8] More recent studies have indicated that copolymers of glycolic acid promoted peripheral nerve regeneration in a rat model.[9,10] These polymers are degraded by hydrolysis and enzymatic activity and have a range of mechanical and physical properties that can be engineered appropriately to suit a particular application.

Knowledge of the biological interactions between chondrocytes and biodegradable polymers is needed to design novel biomaterials and to develop new strategies for cartilage repair. Therefore, further experimental elucidation of these polymers, their combination with other biomaterials, and new materials to find good substrates is essential to attain satisfactory conditions for their clinical application. In this study, along with PGA and poly(L-lactic acid-glycolic acid) (PLGA), we investigated the copolymer poly(glycolic acid-ε-caprolactone) (PGCL), the copolymer poly(L-lactic acid-ε-caprolactone) 75:25 (w/w) P(LA-

CL)25, and poly-ε-caprolactone (tetrabutoxy titanium) [PCL(Ti)] to determine their effects on human articular chondrocyte (HAC) proliferation, differentiation, and phenotypic expression with the aim of clarifying their suitability as carriers for future clinical cartilage transplants. Fullerene C-60 dimalonic acid (DMA) has been reported to stimulate[11] and inhibit[12] proliferation and differentiation of rat embryonic limb bud cells and mouse embryo midbrain cells, respectively, and in the present study we also investigated the effect of fullerene C-60 DMA on HACs.

Gap junctions are intercellular channels supporting direct cell-to-cell communication and tissue integration.[13] Connexins, the family of proteins that form vertebrate gap junctions, play key roles during development and in the adult. Among the 19 connexins that have been identified in mammals, the gap junction protein connexin 43 (Cx43) is the most abundant member of the channel-forming proteins in chondrocytes.[14,15] The distribution of Cx43 in hyaline cartilage and in the perichondrium of mouse and rat knee joints suggested a possible involvement of connexins in cartilage development.[16] It has been indicated that the early stage of in vitro chondrocyte differentiation is the formation of cell condensations and the ability to establish cell-to-cell communication. Cx43, together with other molecular mechanisms, mediates the condensation phase of chondrogenesis.[17] In the present study, we investigated the role of gap junctional protein Cx43 in the process of chondrocyte differentiation.

Materials and methods

Materials

HACs from knee joints and chondrocyte growth medium were commercially obtained from BioWhittaker (Walkersville, MD, USA). Chondrocyte growth medium contains bovine insulin, basic fibroblast growth factor, insulin-like growth factor-1, transferrin, gentamicin sulfate, and fetal bovine serum (5% v/v). PGA (mw 3000) and PLGA (mw 5000) were purchased from Nakalai Tesque (Kyoto, Japan) and PGCL (mw 3000) was from Taki Chemical (Hyogo, Japan). P(LA-CL)25 (mw 10000) and PCL(Ti) (mw 130000) were synthesized in our laboratory and fullerene C-60 DMA was obtained from Dr. T. Mashino.[18]

Synthesis of P(LA-CL)25

L-Lactide (Tokyo Kasei Kogyo, Tokyo, Japan) 7.5g and caprolactone (Wako Pure Chemical Industries, Osaka, Japan) 2.5g were put into a reactor as monomers. As a catalyst, tetrabutoxy titanium (Wako) 0.03g was added. Furthermore, *n*-octyl alcohol (Wako) 0.001g was added. These were completely dissolved in methylene chloride (Wako) 50mL at room temperature. Methylene chloride was removed by decompression and a uniform mixture was left. The reactor was filled with nitrogen and was sealed. The contents were mixed and heated to 140°C. Polymerization was carried out for 4h. After the reaction, the reactant was cooled to room temperature, and was dissolved in tetrahydrofuran 100mL. The solution was dropped into cold methanol and a colorless precipitate was obtained. This was dried under reduced pressure and precipitation was done once again. This was again dried under reduced pressure and the polymer was obtained. The yield was 58.2% (5.82g).

Synthesis of PCL(Ti)

Synthesis was done using the same method as described for the synthesis of P(LA-CL)25 except that the monomer was only caprolactone (Wako). The yield was 87.1% (8.71g).

Preparation of materials

PGA, PGCL, PLGA, and P(LA-CL)25 were dissolved in dimethyl sulphoxide (DMSO) at a concentration of 50μg/0.8μl of DMSO (Sigma-Aldrich, Irvine, CA, USA) and then dissolved in chondrocyte growth medium to give a final concentration of 50μg/ml. PCL(Ti) was dissolved in tetrahydrofran (THF) at a concentration of 5mg of PCL/ml of THF. Glass wells were coated with this solution to give a final concentration of 2mg PCL(Ti)/well. A homogenous solution of fullerene C-60 DMA was made with the chondrocyte growth medium.

Cell culture

In vitro high-density micromass cultures of HACs were initiated by spotting 4×10^5 cells in 20μl of medium onto each well of 12-well microplates for tissue culture (Costar Type 3513, Corning, Corning, NY, USA) and PCL(Ti)-coated glass wells (diameter 22mm). After 2h in a 5% CO_2 incubator at 37°C, the wells were flooded with chondrocyte growth medium (2ml/well). The medium was supplemented with DMSO (0.8μl/ml), PGA (50μg/ml), PGCL (50μg/ml), PLGA (50μg/ml), P(LA-CL)25 (50μg/ml), or fullerene C60 DMA (50μg/ml). HACs cultured on tissue culture polystyrene but not exposed to any biomaterials served as a control. The media were changed in every 3 days and culture was continued for 4 weeks.

Cell morphology assay

Cell morphology was determined by inverted light microscopy. Twice weekly observations were done and photographs were taken with Fuji film.

Proliferation assay

Cell proliferation was quantitatively measured by alamar blue (Biosource International, Camarillo, CA, USA) assay after 4 weeks of culture, as previously described.[18] The assay

demonstrates the metabolic activity of the cells by detection of mitochondrial activity. The indicator dye alamar blue is incorporated into the cells and reduced and excreted as a fluorescent product. At the end of the 4-week culture period, the medium from all wells was discarded and the culture wells and three blank wells were filled with 1 ml/well of 5% alamar blue solution in fresh medium. The culture plates were incubated at 37°C for 4 h. After the incubation period, two aliquots of 100 µl of solution from each well were transferred to new wells of a Costar 96-well tissue culture microplate (Costar Type 3595, Corning). The extent of cell proliferation was quantitated by a Cytofluor II fluorescence multiwell cell reader (PerSeptive Biosystems, Framingham, MA, USA) at 535 nm for excitation and 590 nm for emission. The intensity of the blue color obtained was directly proportional to the metabolic activity of the cell populations. Blank values were subtracted from experimental values to eliminate background readings.

Proteoglycan production assay

Proteoglycans are typical components of the cartilage matrix. The extent of chondrogenesis was determined by staining the cartilage-specific proteoglycans with alcian blue (Wako) as described previously.[11,19] Briefly, the cultures and three blank wells were stained overnight at 4°C (0.5 ml/well) with 1% (v/v) alcian blue, pH 1.0. The alcian blue solution was then removed and the micromass cultures and blank wells were rinsed with 3% (v/v) acetic acid and distilled water to completely remove the free dye. The cartilage proteoglycans were extracted using 4-M guanidine hydrochloride, and the absorbance was measured at a wavelength of 600 nm using an enzyme-linked immunosorbent assay (ELISA) reader (Bio-Tek Instruments, Winooski, VT, USA). Blank values were subtracted from experimental values to eliminate background readings.

RNA harvest

After the 4-week culture period, RNA was extracted from all matrices except the PCL(Ti) matrix. For the PCL(Ti) matrix, we did not have enough samples to harvest RNA because cells from 50% of the cultured wells became detached overnight following cell spotting. Total cellular RNA was extracted from cultured cells of four wells (for each material) in 0.5 ml Trizol reagent (Life Technologies, Frederick, MD, USA) according to the manufacturer's instructions. The concentration of total RNA was determined using a UV spectrophotometer (Gene Quanta, Pharmacy Biotech, Piscataway NJ, USA) at 260 nm.

Reverse transcription (RT) and polymerase chain reaction (PCR)

The matrix molecules probed as part of this study were collagen type II and aggrecan. The gap junction protein gene Cx43 was also studied. Single-strand cDNA was prepared from 1 µg of total RNA by reverse transcription (RT) using a commercially available First-Strand cDNA synthesis kit (Amersham Pharmacia Biotech, Uppsala, Sweden). After optimization of PCR conditions, subsequent PCR was performed with 4 µg of cDNA in a 20-µl reaction mixture (10 × PCR buffer 2 µl, dNTP 1.6 µl, forward and reverse primer 0.4 µl, Taq DNA polymerase 0.1 µl, and distilled water to make up 20 µl). The codon sequence used for the primer sets was as follows:

Collagen type II:
forward 5′-GGCAATAGCAGGTTCACGTACA-3′
reverse 5′-CGATAACAGTCTTGCCCCACTT-3′

Aggrecan:
forward 5′-TCGAGGACAGCGAGGCC-3′
reverse 5′-TCGAGGGTGTAGCGTGTAGAGA-3′.
Connexin 43 (*Homo sapiens*):
forward 5′-ATGGGTGACTGGAGCGCCTTAGGCAA ACTC-3′
reverse 5′-GACCTCGGCCTGATGACCTGGAGATC TAG-3′

For collagen type II and Cx43, an initial denaturation step at 94°C was carried out for 5 min, followed by 40 cycles of 94°C for 1 min, 60°C for 1 min, and 72°C for 1 min, with a final extension at 72°C for 10 min. For aggrecan, an initial denaturation at 95°C was carried out for 10 min, followed by 40 cycles of 95°C for 15 s, 60°C for 1 min, and 72°C for 1 min), with a final extension at 72°C for 5 min. The polymerization of glyceraldehyde-3-phosphate dehydrogenase (GAPDH) was accomplished by 25 cycles with a corresponding PCR program. Electrophoresis of PCR products was done on 3% agarose gel for visualization of collagen type II and aggrecan and on 1% agarose gel for Cx43 after staining with SYBR Green I (BioWhittaker Molecular Applications, Rockland, ME, USA). The relative intensity of signals from each lane was analyzed with a computerized scanner. For relative quantitation, the signal intensity of each lane was standardized to that of a housekeeping gene, GAPDH:

forward 5′-CCCATCACCATCTTCCAGGAGCGAGA-3′
reverse 5′-TGGCCAAGGTCATCCATGACAACTTTG G-3′.

Statistical analysis

Comparing the control with samples exposed to various materials assessed the statistical significance of the cell proliferation and cartilage proteoglycans production. Student's t test was used to assess the statistical significance. Statistical significance was taken as $P < 0.05$. Data were indicated as the mean ± SD (standard deviation). Four or five cultures were run for each biomaterial. All experiments were repeated at least twice, and similar results were obtained.

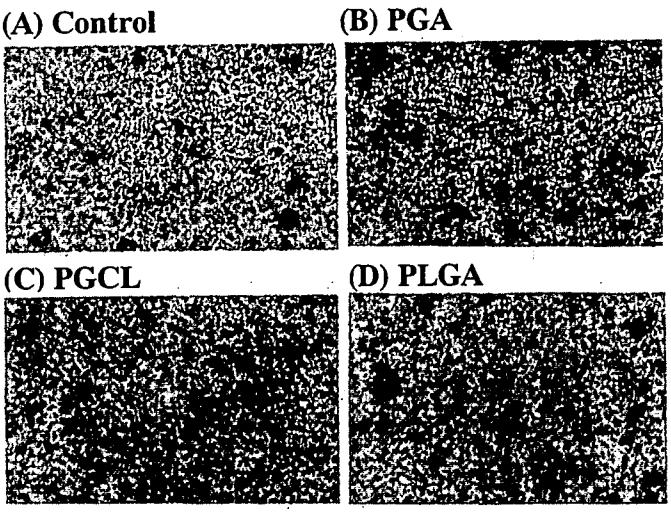

Fig. 1A–D. Light microscopic appearance of cultured human articular chondrocytes spotted as a high-density micromass culture with different biodegradable polymers for 4 weeks. **A** Control, **B** polyglycolic acid (PGA), **C** poly(glycolic acid-ε-caprolactone) (PGCL), **D** poly(L-lactic acid-glycolic acid) (PLGA). Original magnification ×200

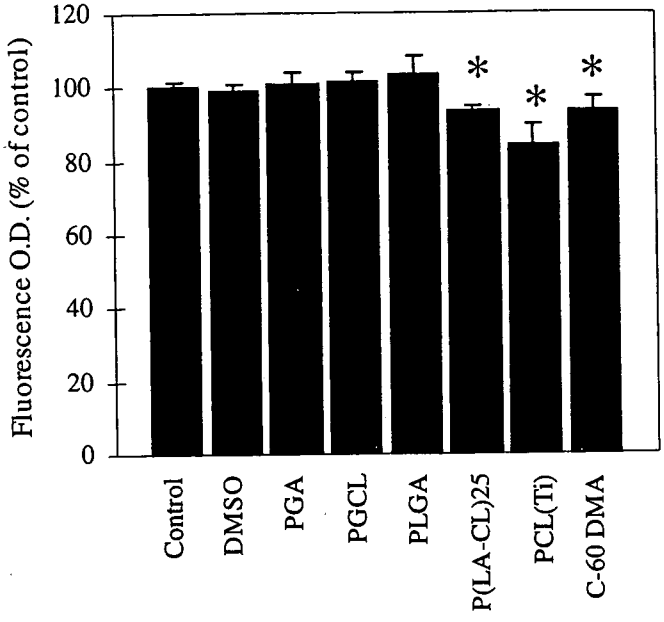

Fig. 2. Cell proliferation of human articular chondrocytes as determined by alamar blue assay after culturing with synthetic biodegradable polymers for 4 weeks. The proliferation in all samples exposed to dimethyl sulfoxide (*DMSO*) and biomaterials were calculated as a percentage of control values. *P(LA-CL)25*, poly(L-lactic acid-ε-caprolactone) 75:25 (w/w); *PCL(Ti)*, poly-ε-caprolactone (tetrabutoxy titanium); *C-60 DMA*, fullerene C-60 dimalonic acid. $*P < 0.05$ and *error bars* represent standard deviations of the mean

Results

Cell morphology

Cells were aggregated as high-density micromass cultures 2h after cell spotting. After 4 weeks of culture, the chondrocytes mainly formed a uniform sheet of chondrogenic cells with nodules. The cartilage nodules were first observed in the first week of the culture. These nodules were better visualized by staining the proteoglycans with alcian blue after 4 weeks of culture. The control cells showed less nodule formation and they were poorly defined (Fig. 1A). The cultures exposed to the PGA and PLGA had more distinct nodules and greater numbers of nodule formations than the controls (Figs. 1B and 1D). The nodules formed in the culture exposed to PGCL were less distinct and fewer in number than the nodules in the cultures exposed to PGA and PLGA, but were more distinct and numerous than the nodules of the control cultures (Fig. 1C). After alcian blue staining, light microscopic examination also revealed that PGA-, PGCL-, and PLGA-treated cultures contained denser extracellular matrix (ECM) than the controls. Cells extended from the edge of all micromass cultures, and the extending cells were spindle-shaped.

Cell proliferation assay

The proliferation rates of all the matrices are shown in Fig. 2, with error bars representing the standard deviation of the mean. All values for the samples exposed to the biomaterials were expressed as a percentage of the control average value, which was taken as 100%. The effect of DMSO on cell proliferation was not significant (99.3% ± 1.6%). The cell proliferations for PGA, PGCL, and PLGA were fairly parallel to that of control cell proliferation. The cell proliferation for P(LA-CL)25, PCL(Ti), and fullerene C-60 DMA were significantly inhibited compared to the control. The inhibitions for P(LA-CL)25 and fullerene C-60 DMA were mainly due to the small variation of the standard deviation. Despite being significantly different from the control, both proliferation values were fairly close to the control proliferation value.

Therefore, from the standpoint of cell proliferation, all materials except for PCL(Ti) remained viable candidates for tissue engineering. The values of cell proliferation for the samples exposed to PGA, PGCL, PLGA, P(LA-CL)25, PCL(Ti), and fullerene C-60 DMA were 101% ± 2.7%, 101.6% ± 2.2%, 103.5% ± 4.8%, 93.2% ± 1.4%, 84.3% ± 5.1%, and 93.6% ± 3.7%, respectively.

Proteoglycan synthesis

The proteoglycans bound with alcian blue were extracted with 4-M guanidine hydrochloride. Their levels were expressed as a percentage of the average control value, which was taken as 100% (Fig. 3). The intensity of alcian blue staining was found to be higher in PGA-, PGCL-, and PLGA-containing cultures than in the control culture. Among the biomaterials, PGA caused a significant 3.1-fold increase in cartilage proteoglycans compared to the control ($P < 0.05$). The samples exposed to PGCL (116.2% ± 10.1%) and PLGA (128.4% ± 11.1%) also produced

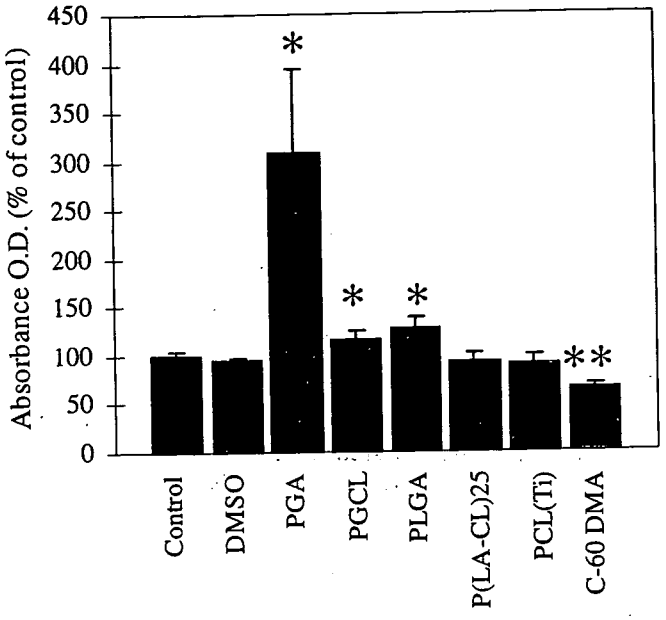

Fig. 3. Cartilage proteoglycan content of human articular chondrocytes as determined by the alcian blue staining method after culturing with synthetic biodegradable polymers for 4 weeks. The values are expressed as a percentage of control values. $^{*}P < 0.05$ and $^{**}P < 0.01$

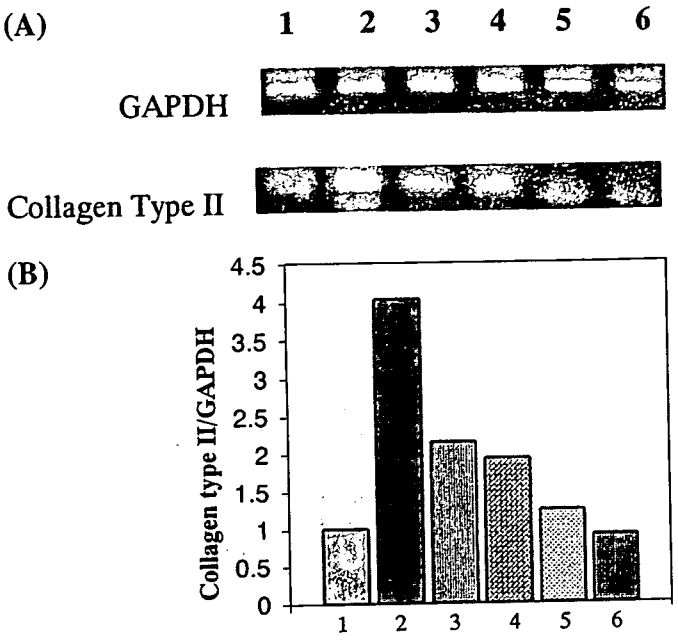

Fig. 4. Reverse transcription polymerase chain reaction (RT-PCR) analysis (**A**) and National Institutes of Health (NIH) image analysis quantitation of RT-PCR bands (**B**). In both figures, the level of collagen type-II gene expression was represented by the mRNA level of 4-week cultured human articular chondrocytes treated with different types of biodegradable polymers. The mRNA expression of housekeeping gene glyceraldehyde-3-phosphate dehydrogenase (*GAPDH*) was used for comparing the level of expression. **A** Lane 1, Control; lane 2, PGA; lane 3, PGCL; lane 4, PLGA; lane 5, P(LA-CL)25; lane 6, Fullerene C-60 DMA. **B** Bar 1, Control; bar 2, PGA; bar 3, PGCL; bar 4, PLGA; bar 5, P(LA-CL)25; bar 6, Fullerene C-60 DMA

significantly higher cartilage proteoglycans than the control. Copolymers P(LA-CL)25 (92.7% ± 10.5%) and PCL(Ti) (90.8% ± 9.1%) did not induce significant changes in cartilage proteoglycans compared to the control. Fullerene C60 DMA acted as a potent inhibitor (66.1% ± 4.7%) and caused a significant inhibition of cartilage proteoglycans ($P < 0.01$) compared to the control. The effect of DMSO (96% ± 1.1%) on cell differentiation was negligible.

Extracellular matrix gene expression

RT-PCR and corresponding National Institutes of Health (NIH) image analysis showed that all matrices consistently supported the expression of the collagen type II gene and that the PGA matrix had the strongest induction (Fig. 4). Slight increases in expression of the collagen type II gene were noted with PGCL, PLGA, and P(LA-CL)25 matrices. Expression of the collagen type II gene for fullerene C60 DMA was similar to the control. The PGA matrix also showed the strongest induction of the aggrecan gene (Fig. 5). Aggrecan gene expression was slightly increased in PGCL and PLGA matrices. The P(LA-CL)25 matrix caused an expression of this gene similar to that of the control, but the fullerene C60 DMA matrix caused decreased expression of this gene.

Expression of gap junction protein connexin 43 gene

To determine the expression of gap junctions during in vitro chondrocyte differentiation, RT-PCR and corresponding

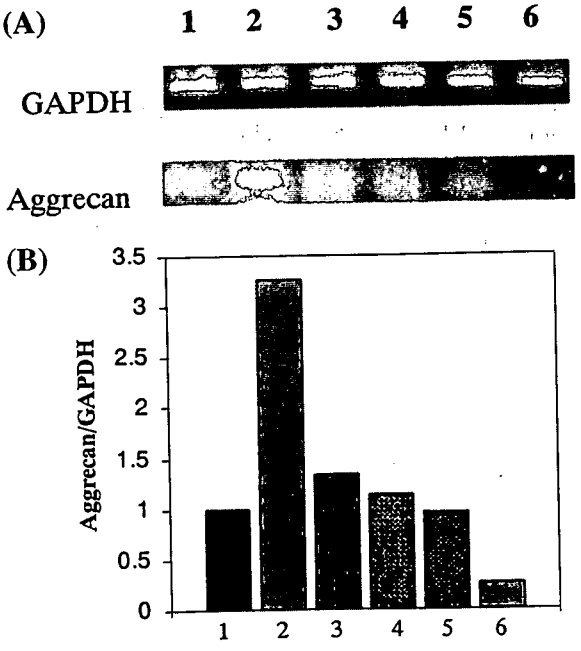

Fig. 5. RT-PCR analysis (**A**) and National Institutes of Health (NIH) image analysis quantitation of RT-PCR bands (**B**). In both figures, the level of aggrecan gene expression was represented by the mRNA level of 4-week cultured human articular chondrocytes treated with different types of biodegradable polymers. The mRNA expression of housekeeping gene GAPDH was used for comparing the levels of expression. *Lanes* and *bars* as defined in Fig. 4

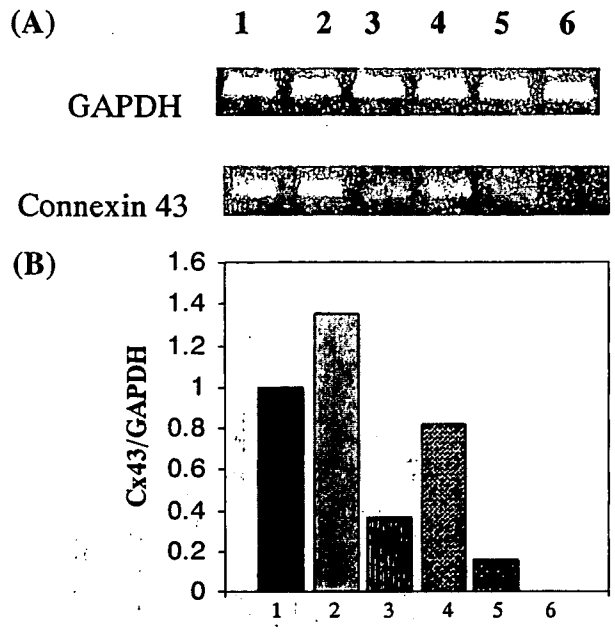

Fig. 6. RT-PCR analysis (**A**) and National Institutes of Health (NIH) image analysis quantitation of RT-PCR bands (**B**). In both figures, the level of connexin 43 gene expression was represented by the mRNA level of 4-week cultured human articular chondrocytes treated with different types of biodegradable polymers. The expression of GAPDH mRNA was used as an internal control. *Lanes* and *bars* as defined in Fig. 4

NIH image analysis was performed with connexin 43 in 4-week cultured human articular chondrocytes treated with various biodegradable biomaterials. Cx43 expression was normalized by comparison to the expression of GAPDH. Figure 6 shows that PGA induced the highest level of Cx43 mRNA expression, and a decreased level of expression was noted in the PLGA- and PGCL-treated cultures. A faint expression for P(LA-CL)25- and almost zero expression for fullerene C-60 DMA-treated cultures were observed.

Multiple regression analysis

Using multiple regression analysis, the correlation was investigated between cartilage proteoglycan production by the alcian blue method and the three gene expression levels. There was a high correlation between cartilage proteoglycan production and the three gene expression levels (data not shown).

Discussion

The evolution of new biodegradable polymers has drawn much attention in recent years, mainly because of growing application in clinical use. PCL is being utilized for biomedical applications such as controlled drug delivery systems[20] and also as surgical implants in rabbits.[21] Just as for PGA and PLLA, PCL degrades to a naturally occurring metabolite, 6-hydroxyhexanoic acid. To date, research to improve materials and the bioactivity of materials for tissue engineering has centered on PGA and PLLA; however, a short resorption time and low strength characteristics are two major drawbacks of these biodegradable materials. To widen the spectrum of biomaterial choices in tissue engineering, we investigated a copolymer of PGA and PCL, namely, PGCL, and copolymers of PLLA and PCL namely, P(LA-CL)25, PCL(Ti), and fullerene C60 DMA. To compare the bioactivity of these materials with commonly used materials, PGA and PLGA were included in this study. We also included PCL(Sn), synthesized using stannous 2-ethyl hexanoate as the catalyst, in our initial study, but following overnight culture after cell spotting, the cells were detached as a white condensed mass from 15 of 16 PCL(Sn)-coated glass wells in repeated studies. Therefore, PCL(Sn) was excluded from this study. Cells were also detached from 8 (50%) of a total of 16 glass wells coated with PCL(Ti). Thus, both PCL(Ti) and PCL(Sn) matrices were harmful to the cell attachment process. Decreased attachment of human articular chondrocytes with PCL matrix was previously reported.[22] After culture periods of 4 weeks, cell proliferation was significantly inhibited by the PCL(Ti) matrix, and together with its poor cell attachment ability, this ruled out PCL(Ti) as a matrix for future chondrocyte culture. The significant inhibition of cell proliferation by P(LA-CL)25 and fullerene C60 DMA matrices was a result of their narrow range of standard deviation, but, with proliferation levels of 93% of that for the control, they remain feasible candidates for tissue engineering biomaterials. Other matrices had comparable cell proliferation to the control.

During differentiation, chondrocytes secrete extracellular matrix (ECM) molecules characteristic of cartilage, such as type II collagen, aggrecan, and link protein, offering an environment that preserves the chondrocyte phenotype. Therefore, chondrocytes are defined both by their morphology and their ability to produce these characteristic ECM molecules. Collagen type II is regarded as the most important component among the ECM molecules. Previous study detected type II collagen as early as 7 days after beginning 3-D culture, and at 21 days, the matrix of the entire aggregate contained type II collagen.[23] Among the ECM molecules, aggrecan is a major proteoglycan.[24] It has been reported that in chick cartilage, aggrecan expression starts at embryonic day 5 in limb rudiments, continues through the entire period of chondrocyte development, and remains a biochemical marker of the cartilage phenotype thereafter.[25]

In this study, we demonstrated good cell differentiation with the formation of cartilaginous nodules on culture plates by alcian blue staining, which is commonly used for identification of cartilage, and by expression of ECM molecules collagen type II and aggrecan. The morphology after the designated culture period revealed that cells aggregated on the culture plate and formed cartilaginous nodules (Fig. 1). These nodules were first observed after 1 week of culture and progressively became denser as culture continued. These nodules contained copious amounts of ECM, which became stained intensely with alcian blue. The greatest cell

differentiation, a 3.1-fold increase of that of the controls, was found in the sample treated with PGA. The potencies of cell differentiation after 4 weeks of culture from the highest to the lowest were in the following order: PGA >> PLGA > PGCL > Control = DMSO > P(LA-CL)25 = PCL(Ti) >> fullerene C60 DMA. The increased cell differentiation with PGA and PLGA matrices are in agreement with our previous findings in a micromass culture system;[19] however, in our present study we included the matrix gene expression of these materials. The cell differentiation findings of PCL(Ti) and copolymers PGCL and P(LA-CL)25 could not be compared with other studies because we found no reports describing the effects of PCL and its associated polymers on chondrocyte differentiation. The recent discovery that fullerene C60 DMA can be produced in macroscopic quantities has sparked much interest in the chemistry of this unusual molecule, which did not cause acute toxic effects on mouse skin epidermis.[26] Increased cell proliferation and differentiation of rat embryonic limb bud cells by fullerene C60 were reported,[11] but the data of the present study showed that fullerene C60 DMA acted as a potent inhibitor of HAC differentiation.

As tissue engineering becomes increasingly complex, there is a need to understand how a specific biomaterial influences gene expression. Therefore, the matrices used in this study were evaluated with respect to their influence on the expression of collagen type II and aggrecan genes (Figs. 4 and 5). The increased expression of collagen type II and aggrecan genes in the PGA-, PGCL-, and PLGA-treated matrices was well correlated with their elevated level of cell differentiation values, as shown by alcian blue staining. The low expression of collagen type II and aggrecan genes in the fullerene C60 DMA-treated matrix paralleled the decreased level of cell differentiation, as shown by alcian blue. Therefore, low cell proliferation and differentiation values along with almost no expression of collagen type II and aggrecan genes in the fullerene C60 DMA-treated matrix completely exclude this matrix from use in ECM tissue engineering. The expression of collagen type II and aggrecan genes in the P(LA-CL)25-treated culture was consistent with its cell differentiation value. The data from this study showed that cultured chondrocytes also retained their phenotype throughout the experimental period, as indicated by expression of the type II collagen gene (Fig. 4A, 4B). To the best of our knowledge, this study is the first to show the bioactivity of PCL(Ti) and copolymers PGCL and P(LA-CL)25 in chondrogenic differentiation of HAC in a micromass culture system. Further, we know of no studies that have evaluated the matrix gene expression for PGA and PLGA matrices using HAC in a micromass culture system. Results of the present study confirmed PGA, PLGA, and PGCL as useful scaffolding matrices for cartilage tissue engineering, and information about the other matrices will further contribute to the development of improved cartilaginous constructs for future clinical implants.

The progression of chondrogenic differentiation can be followed by the expression of markers of cytodifferentiation. For example, precartilaginous condensations express type I collagen,[27] whereas the next phase of cartilage differentiation involves the expression of type II collagen, aggrecan, and link proteins, which form the cartilage matrix.[28] The mechanism of precartilaginous condensation is poorly understood, but cell–cell interactions are putative effectors for chondrocyte aggregation.[29] Chondrocytes in the primary culture can proceed through the same differentiation program as they do in the cartilaginous angle of the long bone, and the earliest morphological event on the way to overt differentiation is the formation of cell condensation.[17] The observed expression of Cx43 suggested that the process of condensation is in part caused by the interconnection of cells by means of gap junctions.[13] In this study, RT-PCR analysis showed that the mRNA level of Cx43 gene expression was consistent with chondrogenic differentiation in the presence of different biomaterials. Our findings on Cx43 expression by chondrocytes are in agreement with a previous study that reported expression of functional gap junctions by chondrocytes isolated from adult articular cartilage.[30] Gap junction-mediated intercellular communication is critically involved in the development of cartilage during differentiation.[31]

Conclusions

The analysis of three set of genes, namely collagen type II, aggrecan, and Cx43 was important to evaluate the effect of biodegradable polymers and other types of cartilaginous scaffolds on the chondrogenesis of HAC for tissue engineering.

Acknowledgments We are grateful for the support of Health and Labour Sciences Research Grants, and support from Research on Advanced Medical Technology, Ministry of Health, Labour and Welfare, and the Japan Health Sciences Foundation.

References

1. Taylor MS, Daniels AU, Andriano KP, Heller J. Six bioabsorbable polymers: in vitro acute toxicity of accumulated degradation products. J Appl Biomater 1994;5:151–157
2. Nakamura T, Shimizu Y, Okumura N, Matsui T, Hyon SH, Shimamoto T. Tumorigenicity of poly-L-lactide (PLLA) plates compared with medical-grade polyethylene. J Biomed Mater Res 1994;28:17–25
3. Matsusue Y, Yamamuro T, Oka M, Shikinami Y, Hyon SH, Ikada Y. In vitro and in vivo studies on bioabsorbable ultra-high-strength poly (L-lactide) rods. J Biomed Mater Res 1992;26:1553–1567
4. Furukawa T, Matsusue Y, Yasunaga T, Shikinami Y, Okuno M, Nakamura T. Biodegradation behavior of ultra-high-strength hydroxyapatite/poly (L-lactide) composite rods for internal fixation of bone fractures. Biomaterials 2000;21:889–898
5. Hope PG, Williamson DM, Coates CJ, Cole WG. Biodegradable pin fixation of elbow fractures in children. J Bone Joint Surg 1991;73:965–968
6. Kleinschmidt J, Marden L, Kent D; Quigley N, Hollinger J. A multiphase system bone implant for regenerating the calvaria. J Plast Reconstr Surg 1993;91:581–588
7. Hollinger JO. Preliminary report on the osteogenic potential of a biodegradable copolymer of polylactide (PLA) and polyglycolide (PGA). J Biomed Mater Res 1983;17:71–82

8. Tormala P, Pohjonen T, Rokkanen P. Bioabsorbable osteosynthetic implants of ultra-high-strength poly-L-lactide. A clinical study. Int Orthop 1996;20:392–394
9. Evans GR, Brandt K, Widmer MS, Lu L, Meszlenyi RK, Gupta PK, Mikos AG, Hodges J, Williams J, Gurlek A, Nabawi A, Lohman R, Patrick CW Jr. In vivo evaluation of poly (L-lactic acid) porous conduits for peripheral nerve regeneration. Biomaterials 1999;20:1109–1115
10. Hadlock T, Sundback C, Hunter D, Cheney M, Vacanti JP. A polymer foam conduit seeded with Schwann cells promotes guided peripheral nerve regeneration. Tissue Eng 2000;6:119–127
11. Tsuchiya T, Yamakoshi YN, Miyata N. A novel promoting action of fullerene C60 on the chondrogenesis in rat embryonic limb bud cell culture system. Biochem Biophys Res Commun 1995;206:885–894
12. Tsuchiya T, Oguri I, Yamakoshi YN, Miyata N. Novel harmful effects of [60] fullerene on mouse embryos in vitro and in vivo. FEBS Lett 1996;393:139–145
13. Kumar NM, Gilula NB. The gap junction communication channel. Cell 1996;84:381–388
14. Solursh M, Linsenmeyer TF, Jensen KL. Chondrogenesis from single limb mesenchyme cells. Dev Biol 1982;94:259–262
15. Willecke K, Hennemann H, Dahl E, Jungbluth S, Heynkes R. The diversity of connexin genes encoding gap junctional proteins. Eur J Cell Biol 1991;56:1–7
16. Schwab W, Hofer A, Kasper M. Immunohistochemical distribution of connexin 43 in the cartilage of rats and mice. Histochem J 1998;30:413–419
17. Loty S, Foll C, Forest N, Sautier JM. Association of enhanced expression of gap junctions with in vitro chondrogenic differentiation of rat nasal septal cartilage-released cells following their dedifferentiation and redifferentiation. Arch Oral Biol 2000;45:843–856
18. Okuda K, Hirota M, Hirobe T, Nagano M, Mochizuki M, Mashino T. Synthesis of various water-soluble C60 derivatives and their superoxide-quenching activity. Fullerene Sci Tech 2000;8:89–104
19. Rahman MS, Tsuchiya T. Enhancement of chondrogenic differentiation of human articular chondrocytes by biodegradable polymers. Tissue Eng 2001;7:781–790
20. Hombreiro PM, Zinutti C, Lamprecht A, Ubrich N, Astier A, Hoffman M, Bodmeier R, Maincent P. The preparation and evaluation of poly (epsilon-caprolactone) microparticles containing both a lipophilic and a hydrophilic drug. J Control Release 2000;65:429–438
21. Lowry KJ, Hamson KR, Bear L, Peng YB, Calaluce R, Evans ML, Allen WC. Polycaprolactone/glass bioabsorbable implant in a rabbit humerus fracture model J Biomed Mater Res 1997;36:536–541
22. Ishaug-Riley SL, Okun LE, Prado G, Applegate MA, Ratcliffe A. Human articular chondrocyte adhesion and proliferation on synthetic biodegradable polymer films. Biomaterials 1999;20:2245–2256
23. Johnstone B, Hering TM, Caplan AI, Goldberg VM, Yoo JU. In vitro chondrogenesis of bone marrow-derived mesenchymal progenitor cells. Exp Cell Res 1998;23:265–272
24. Watanabe H, Yamada Y, Kimata K. Roles of aggrecan, a large chondroitin sulfate proteoglycan, in cartilage structure and function. J Biochem (Tokyo) 1998;124:687–693
25. Schwartz NB, Domowicz M, Krueger RC Jr, Li H, Mangoura D. Brain aggrecan. Perspect Dev Neurobiol 1996;3:291–306
26. Nelson MA, Domann FE, Bowden GT, Hooser SB, Fernando Q, Carter DE. Effects of acute and subchronic exposure of topically applied fullerene extracts on the mouse skin. Toxicol Ind Health 1993;9:623–630
27. Langille RM, Solursh M. Formation of chondrous and osseous tissues in micromass cultures of rat frontonasal and mandibular ectomesenchyme. Differentiation 1990;44:197–206
28. Kosher RA, Gay SW, Kamanitz JR, Kulyk WM, Rodgers BJ, Sai S, Tanaka T, Tanzer ML. Cartilage proteoglycan core protein gene expression during limb cartilage differentiation. Dev Biol 1986;118:112–117
29. Frenz DA, Jaikaria NS, Newman SA. The mechanism of precartilage mesenchymal condensation: a major role for interaction of the cell surface with the amino-terminal heparin-binding domain of fibronectin. Dev Biol 1989;136:97–103
30. Donahue HJ, Guilak F, Vander Molen MA, McLeod KJ, Rubin CT, Grande DA, Brink PR. Chondrocytes isolated from mature articular cartilage retain the capacity to form functional gap junctions. J Bone Miner Res 1995;10:1359–1364
31. Coelho CN, Kosher RA. Gap junctional communication during limb cartilage differentiation. Dev Biol 1991;144:47–53

Available online at www.sciencedirect.com
ScienceDirect
Biomaterials 28 (2007) 844–850
Biomaterials
www.elsevier.com/locate/biomaterials

Effects of sulfated hyaluronan on keratinocyte differentiation and Wnt and Notch gene expression

Tsutomu Nagira[a,b], Misao Nagahata-Ishiguro[a], Toshie Tsuchiya[a,*]

[a]*Division of Medical Devices, National Institute of Health Sciences, 1-18-1 Kamiyoga, Setagaya-ku, Tokyo 158-8501, Japan*
[b]*Japan Association for the Advancement of Medical Equipment, 3-42-6 Hongo, Bunkyo-ku, Tokyo 113-0033, Japan*

Received 3 July 2006; accepted 24 September 2006

Available online at www.sciencedirect.com
ScienceDirect
Biomaterials 28 (2007) 844–850
Biomaterials
www.elsevier.com/locate/biomaterials

Effects of sulfated hyaluronan on keratinocyte differentiation and Wnt and Notch gene expression

Tsutomu Nagira[a,b], Misao Nagahata-Ishiguro[a], Toshie Tsuchiya[a,*]

[a]*Division of Medical Devices, National Institute of Health Sciences, 1-18-1 Kamiyoga, Setagaya-ku, Tokyo 158-8501, Japan*
[b]*Japan Association for the Advancement of Medical Equipment, 3-42-6 Hongo, Bunkyo-ku, Tokyo 113-0033, Japan*

Received 3 July 2006; accepted 24 September 2006

Abstract

Sulfated hyaluronan (SHya), which is composed of a sulfated group and hyaluronan (Hya), has high activity on and biocompatibility with cells. When normal human epidermal keratinocytes (NHEKs) were incubated in dishes coated with SHya, cell proliferation was suppressed in a dose-dependent manner. The expression levels of keratin 1 and loricrin mRNAs, as detected by real-time RT-PCR, were increased significantly. The expressions of Wnt mRNAs, which play important roles in cell proliferation and differentiation, were modulated. Wnt4 and Wnt6 mRNA expressions were increased compared to controls, while expression of Wnt5a was similar to the control and that of Wnt7a mRNA was decreased. In addition, the expression of Notch mRNAs, which play a critical role in keratinocyte differentiation, were affected. Notch3 mRNA was increased significantly, while Notch1 mRNA was decreased compared to controls, and expression of Notch2 was similar to that of control. These results suggested that a SHya-coated scaffold might be useful for regulating cell activity in tissue engineering.

Keywords: Sulfated hyaluronan; Normal human epidermal keratinocyte; Differentiation; Wnt; Notch

1. Introduction

Normal human epidermal keratinocytes (NHEKs) are usually cultured on 3T3 mouse feeder-layer cells [1]. Several biomaterials have been developed from other animals or humans, but they carry the risk of infection from prions and viruses [2,3]. In contrast, biomaterials from microorganisms carry lower risks of infection, and the development of a semi-synthetic material promoting cell activity will enable safer cell culture.

Several types of polysaccharides for culturing NHEKs have been studied [4,5]. Hyaluronan (Hya) is a negatively charged glycosaminoglycan that is a major component of the extracellular matrix (ECM) [6,7]. Hya plays important roles in cell adhesion, migration, proliferation, and differentiation [7–9]. Park and Tsuchiya reported that a Hya-coated surface is capable of enhancing gap junctional intercellular communication (GJIC) and differentiation or cell growth [10,11]. Sulfated polysaccharides, such as heparin or heparin sulfate, stabilize some growth factors, resulting in enhancement of their effects [12], and promote their mitogenic activity [13]. Sulfated hyaluronan (SHya), a semi-synthetic material composed of Hya and a sulfate group [14] can be synthesized using Hya extracted from microorganisms; therefore, it has a lower infectivity and a lower risk of containing virus-induced carcinogens.

It has been reported that Hya and chondroitin sulfate A enhanced chondrogenesis of human mesenchymal stem cells [15,16]. We hypothesized that SHya has the potential to function as a biomaterial promoting keratinocyte differentiation because it has been reported that SHya stimulates cell activities [14,17]. Analysis of the effects of SHya on cell differentiation and intercellular signaling will provide the information allowing construction of biomaterials of greater usefulness for tissue engineering.

Wnts are secreted glycoproteins that bind Frizzled receptors and play a critical role in the process of cell differentiation in the canonical pathway. In the canonical

*Corresponding author. Tel.: +81 3 37009196; fax: +81 3 3700 91968.
E-mail addresses: nagira@nihs.go.jp (T. Nagira), tsuchiya@nihs.go.jp (T. Tsuchiya).

0142-9612/$ - see front matter © 2006 Elsevier Ltd. All rights reserved.
doi:10.1016/j.biomaterials.2006.09.041

pathway, beta-catenin stabilized by the binding of Wnt proteins to Frizzled receptors stimulates TCF/LEF transcription. A mouse keratinocyte cell line with decreased Wnt4 expression showed a more malignant morphology and was less differentiated [18], Wnt6 was required for epithelialization of the segmental plate mesoderm [19], and Wnt7a promoted cell proliferation by activation of Rac-GTPase and beta-catenin [20].

Notch receptors play a crucial role in determination of cell fate. Notch1 signaling plays an essential role in regulation of mouse keratinocyte differentiation [21]. In mouse keratinocytes, Notch1 activation suppressed Wnt4 activity mediated by the cyclin/CDK inhibitor p21 (WAF1/Cip1) [22]. Notch3 was required for the differentiation of vascular smooth muscle cells and T-cells [23,24].

In a previous study, we demonstrated that a Hya coating promoted several cell functions better than a Hya-supplemented one [25]. Therefore, in this study, we investigated the effects of a SHya coating on keratinocyte differentiation.

2. Materials and methods

2.1. Sulfated hyaluronan

SHya was prepared by the method reported previously [4]. A solution of 2% Hya120 (molecular weight, 1.2×10^6) solution in *N,N*-dimethylformamide (DMF) (Wako Pure Chemical Industries, Ltd., Osaka, Japan) was mixed with trimethylamine (TMA)–SO_3 complex (Aldrich Chemical Co., Inc., Milwaukee, WI, USA) and stirred for 24 h at 60 °C. The reaction mixture was then diluted, neutralized, and precipitated by adding a large quantity of acetone (Wako Pure Chemical Industries). The precipitate was dissolved in distilled water and dialyzed against distilled water. The molecular weight of SHya was 2.0×10^5, and the degree of substitution (D.S.) of SHya was 1.0, as determined by the chelate titration method [26] (Fig. 1). Moreover, the effectiveness of sulfation was also demonstrated by FT-IR analysis. The IR spectrum of SHya exhibited two absorption bands at 1240 and 820 cm^{-1} due to S=O and SO_3^- stretching, respectively.

2.2. Cell culture

NHEKs isolated from neonatal human foreskins (Cambrex Bioscience, Walkersville, MD, USA) were cultured with K-110 Type II medium (Kyokuto, Tokyo, Japan) supplemented with 2% whole bovine pituitary extract, 50 IU penicillin G, 50 μg/ml streptomycin, and 0.03 mM $CaCl_2$ (low-calcium condition) at 37 °C in a humidified atmosphere of 5% CO_2 and 95% air. Keratinocyte differentiation was induced in 0.20 mM $CaCl_2$ medium (high-calcium condition). The medium was exchanged for a fresh one every 2 days.

2.3. Preparation of SHya-coated culture dishes and well plates

Both 35 and 100 mm polystyrene dishes (Iwaki, Funabashi, Japan) and 24-well plates (Corning, Corning, NY, USA) were coated with SHya dissolved in distilled water at a final density of 0.4 or 0.8 mg/cm^2. The SHya-coated dishes and plates were dried under a sterile airflow at room temperature for 8 h.

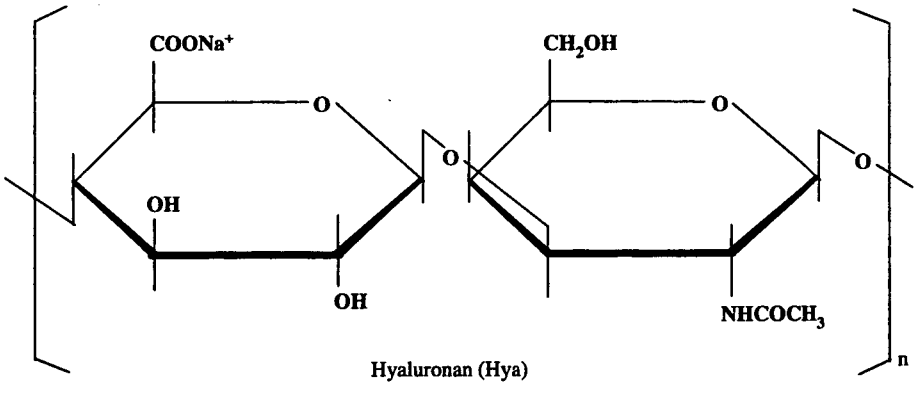

Hyaluronan (Hya)

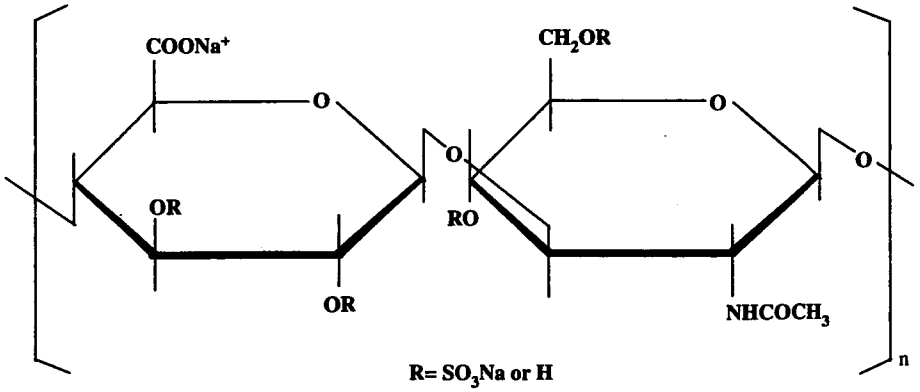

R= SO_3Na or H

Sulphated hyaluronan (SHya)

Fig. 1. The structures of hyaluronan and sulfated hyaluronan. Sulfated hyaluronan (SHya) is composed of Hya and a sulfate group. The molecular weight of SHya is 2.0×10^5, and the degree of substitution of SHya was 1.0.

2.4. Determination of cell numbers by crystal violet assay

NHEKs were seeded at 1.0×10^4 cells/cm^2 in wells of 24-well plates coated with various concentrations of SHya (0, 0.4, and 0.8 mg/cm^2) and incubated in the high-calcium condition (0.20 mM) for 5 days. After washing with Ca^{2+}, Mg^{2+}-free phosphate-buffered saline [PBS(−)], cells were exposed to 0.4% crystal violet (Wako) in methanol for 15 min. NHEKs were washed with PBS(−) three times and destained with 500 μl of methanol for 20 min. Then, absorbance was read at 590 nm using a plate reader.

2.5. Quantitative real time RT-PCR

NHEKs were seeded at 1.0×10^4 cells/cm^2 in various concentrations on SHya-coated 60 mm dishes (0, 0.4, and 0.8 mg/cm^2) and incubated in the high-calcium condition (0.20 mM) for 5 days. Cells were washed with PBS(−) three times, and total RNA was extracted from NHEKs using an RNeasy mini kit (Qiagen, Valencia, CA, USA) according to the manufacturer's instructions. RNA was reverse transcribed into 10 μl DNA using an ExScript RT reagent kit (Takara Co., Ltd., Tokyo, Japan) according to the manufacturer's instructions. Aliquots of the cDNA were used as templates for PCR analysis using a Lightcycler system (Roche, Mannheim, Germany). PCR amplification was performed in a total volume of 20 μl including 1 μl of RT reaction, 10 μl of SYBR *Premix Ex Taq* (Takara), and 0.4 μM/l of each primer. The PCR reaction was performed as follows: 40 cycles of 95 °C for 10 s, 60 °C for 20 s, and 65 °C for 15 s. The PCR primers were purchased from Takara Co., Ltd. The PCR primer sequences for amplification of keratin 1 were forward primer 5′-AGATCACTGCTGGCAGACATGG-3′, and reverse primer 5′-TGATGGACTGCTGCAAGTTGG-3′. The PCR primer sequences for amplification of loricrin were forward primer 5′-TCATGATGC-TACCCGAGGTTTG-3′, and reverse primer 5′-CAGAACTAGATG CAGCCGGAGA-3′. The PCR primer sequences for amplification of Wnt4 were forward primer 5′-CCAGCAGAGCCCTCATGAAC-3′, and reverse primer 5′-TCCACCTCAGTGGCACCATC-3′. The PCR primer sequences for amplification of Wnt6 were forward primer 5′-CTG GAATTGCTCCAGCCACA-3′, and reverse primer 5′-GCAGTGAT GGCGAACACGA-3′. The PCR primer sequences for amplification of Wnt7a were forward primer 5′-GCCCGGACTCTCATGAACTTG-3′, and reverse primer 5′-CCTCGTTGTACTTGTCCTTGAGCA-3′. The PCR primer sequences for amplification of Notch1 were forward primer 5′-TGCGAGGTCAACACAGACGAG-3′, and reverse primer 5′-GTG TAAGTGTTGGGTCCGTCCAG-3′. The PCR primer sequences for amplification of Notch2 were forward primer 5′-TGAACACTGGGTC GATGATGAAG-3′, and reverse primer 5′-AGCGATGGTGTCC TACGGATG-3′. The PCR primer sequences for amplification of Notch3 were forward primer 5′-TGATGGCATGGATGTCAATGTG-3′, and reverse primer 5′-CAGTTGGCATTGGCTCCAGA-3′. The PCR primer sequences for amplification of GAPDH were forward primer 5′-GCACCGTCAAGGCTGAGAAC-3′, and reverse primer 5′-ATGG TGGTGAAGACGCCAGT-3′. Each sample was tested in triplicate.

2.6. Statistical analysis

Significant differences between groups were evaluated with Student's *t*-test. Mean differences were considered significant when $^{**}p < 0.01$. Three samples were run for each case. All experiments were repeated at least twice, and similar results were obtained.

3. Results

3.1. Adhesiveness of NHEKs to SHya

Normal human dermal fibroblasts showed low adhesion to Hya-coated surfaces [9,10]. In order to assess the adhesion of NHEKs to SHya-coated surfaces, NHEKs were seeded on SHya- and Hya-coated surfaces (0, 0.4, and 0.8 mg/cm^2). Fig. 2 shows that NHEKs adhered to SHya-coated surfaces as well as to an uncoated dish, but they did not adhere to the Hya-coated dishes.

3.2. Effect of SHya coating on keratinocyte proliferation

NHEKs were seeded on SHya-coated dishes (0.4 or 0.8 mg/cm^2) and incubated in a high-calcium condition

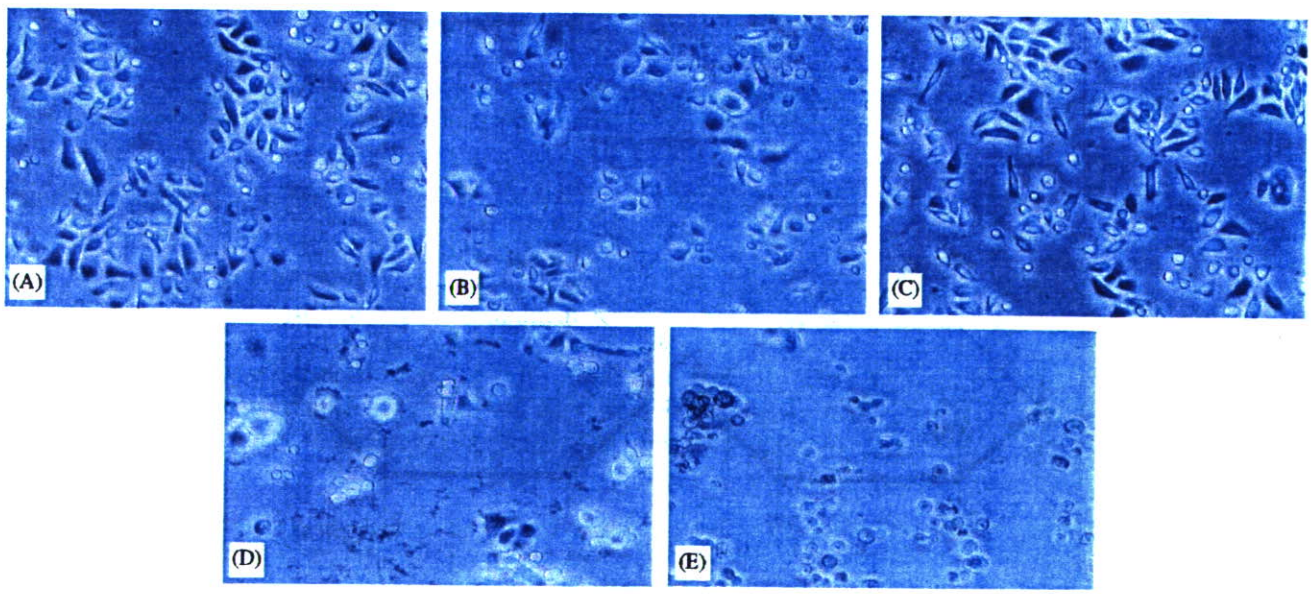

Fig. 2. The adhesion of NHEKs to SHya-coated surfaces. NHEKs were seeded at 1.0×10^4 cells/cm^2 onto SHya- and Hya-coated 24-well plates. Then NHEKs were incubated with non-coated (A), 0.4 mg/cm^2 SHya-coated (B), 0.8 mg/cm^2 SHya-coated (C), 0.4 mg/cm^2 Hya-coated (D), and 0.8 mg/cm^2 Hya-coated (E) wells for 16 h.

(0.20 mM) for 5 days. The cell proliferation assay showed that the SHya coating suppressed keratinocyte proliferation remarkably in a dose-dependent manner (Fig. 3).

3.3. Effect of SHya coating on keratin1 and loricrin expression

To ensure that the SHya coating promoted keratinocyte differentiation, we detected the relative expression levels of differential marker mRNA by real-time RT-PCR. After NHEKs were incubated with SHya coating in a high-calcium condition (0.20 mM) for 5 days, the expression level of keratin1 mRNA on NHEKs was increased more than eight-fold compared to the control (Fig. 4A) and that of loricrin mRNA was increased in a dose-dependent manner (Fig. 4B).

3.4. Effect of SHya coating on Wnts expressions

The expression levels of Wnt4 and Wnt6 mRNA on NHEKs incubated with SHya coating in the low-calcium condition were measured (Fig. 5A and B); the expression level of Wnt5a of NHEKs incubated with SHya coating was decreased to 95% of the control (Fig. 5C) and that of Wnt7a mRNA to about 40% of the control (Fig. 5D).

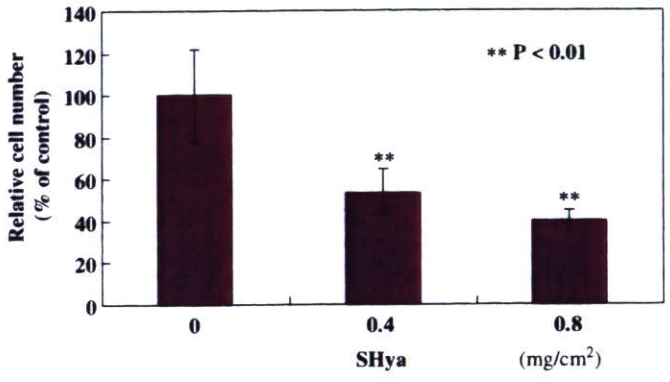

Fig. 3. Suppressive effect of SHya on keratinocyte proliferation. NHEKs were seeded at 1.0×10^4 cells/cm^2 densities onto non-coated (A), 0.4 mg/cm^2 SHya-coated (B), and 0.8 mg/cm^2 SHya-coated (C) 24-well plates and cultured for 5 days. Then numbers of NHEKs were determined by crystal violet assay. Each value is expressed as the mean ± SD. $^{**}P < 0.01$ compared to control.

3.5. Effect of SHya coating on Notch expressions

The expression level of Notch1 mRNA on NHEKs incubated with SHya coating was decreased about 75% compared to the control, and that of Notch2 mRNA was similar to the control (Fig. 6A and B). However, the expression level of Notch3 mRNA was increased about eight-fold compared to the control (Fig. 6C).

4. Discussion

Several studies have suggested that SHya interacts with cells [4], but the effect of SHya on cell differentiation and intercellular signaling was not clear. We demonstrated that a SHya coating promoted keratinocyte differentiation and modulated the expression levels of Notch and Wnt mRNAs.

In this study, the expression levels of Wnt4 and Wnt6 on NHEKs incubated with SHya were increased. A mouse keratinocyte cell line with a deficit of Wnt4 expression showed less differentiation [18]. Wnt6 regulated epithelization [19], suggesting that the SHya-induced upregulation of Wnt4 and Wnt6 is associated with the regulation of keratinocyte differentiation. Wnt7a promoted cell proliferation in corneal epithelial cells during wound healing [20], suggesting that SHya down-regulated Wnt7a expression, resulting in the enhancement of keratinocyte differentiation. The activation of beta-catenin, a downstream factor of Wnt signaling, contributes to keratinocyte differentiation [27]. A sulfated proteoglycan-induced Wnt-11 expression in mouse kidney cells, and sulfated polysaccharides were required in Wnt signaling in mouse kidney cells [28,29]. Therefore, it was suggested

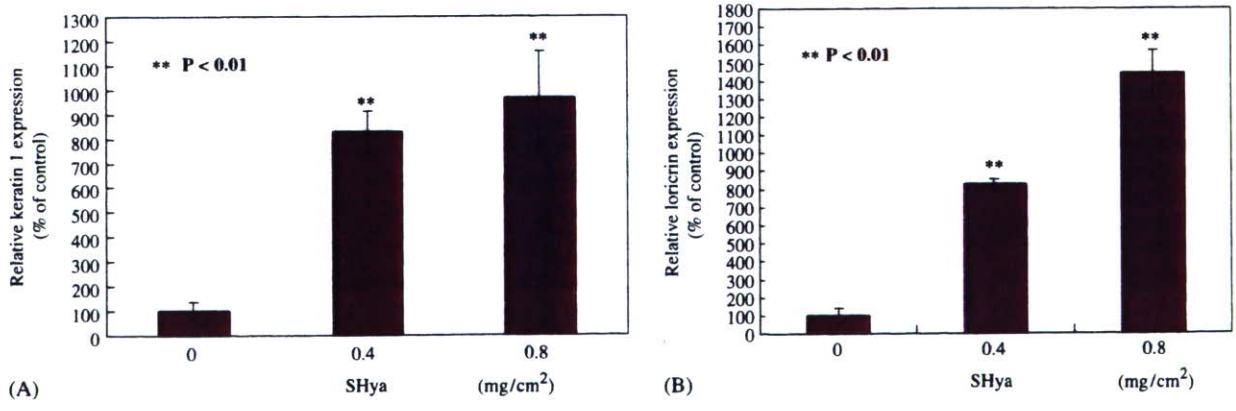

Fig. 4. The expression levels of keratin1 and loricrin mRNA of NHEKs incubated with SHya coating. NHEKs were seeded at 1.0×10^4 cells/cm^2 onto SHya-coated 60 mm dishes (0, 0.4, and 0.8 mg/cm^2) and cultured in medium with 0.20 mM calcium for 5 days. Then RNA was extracted, and real-time RT-PCR was performed to determine the expression levels of keratin1 and loricrin mRNA. Effect of SHya on the expression level of (A) keratin1 mRNA, and (B) loricrin mRNA. Each value is expressed as the mean ± SD. $^{**}P < 0.01$ compared to control.